ADVANCED ENERGY MATERIALS
www.advenergymat.de

Thermodynamic Aspects of Cathode Coatings for Lithium-Ion Batteries

*Muratahan Aykol, Scott Kirklin, and C. Wolverton**

Metal oxide cathode coatings are capable of scavenging the hydrofluoric acid (HF) (present in $LiPF_6$-based electrolytes) and improving the electrochemical performance of Li-ion batteries. Here, a first-principles thermodynamic framework is introduced for designing cathode coatings that consists of four elements: i) HF-scavenging enthalpies, ii) volumetric and iii) gravimetric HF-scavenging capacities of the oxides, and iv) cyclable Li loss into coating components. 81 HF-scavenging reactions involving binary s-, p- and d-block metal oxides and fluorides are enumerated and these materials are screened to find promising coatings based on attributes (i-iv). The screen successfully produces known effective coating materials (e.g., Al_2O_3 and MgO), providing a validation of our framework. Using this design strategy, promising coating materials, such as trivalent oxides of d-block transition metals Sc, Ti, V, Cr, Mn and Y, are predicted. Finally, a new protection mechanism that successful coating materials could provide by scavenging the wide bandgap and low Li ion conductivity LiF precipitates from the cathode surfaces is suggested.

1. Introduction

A key challenge for many Li-ion battery cathodes is to retard the decay of their electrochemical performance and extract capacities close to the theoretical limits over many cycles.[1,2] Dissolution of the redox-active metal[3,4] from the cathode particles is one of the primary reasons for the capacity fade often observed in these materials. This dissolution is enhanced in the presence of the highly corrosive hydrofluoric acid (HF) continuously produced by degradation of the common $LiPF_6$-based electrolytes.[4–7] The degradation reaction of $LiPF_6$ can be written in the form,[4–7]

$$LiPF_6 \rightarrow LiF\downarrow + PF_5 \quad (1)$$

Solid LiF, which has a low permeability to Li-ions[8,9] and electrons,[10] precipitates (↓) on the electrode particles, and PF_5 further reacts with any trace amount of water to produce HF as,

$$PF_5 + H_2O \rightarrow 2HF + POF_3 \quad (2)$$

M. Aykol, S. Kirklin, Prof. C. Wolverton
Department of Materials Science and Engineering
Northwestern University
Evanston, IL 60208, USA
E-mail: c-wolverton@northwestern.edu

DOI: 10.1002/aenm.201400690

The widely utilized polyvinylidene fluoride binder also contributes to the production of HF and subsequent redox-active metal dissolution in Li-ion batteries.[11]

Suppression of the dissolution of redox-active metal is a vitally important goal for capacity retention in Li-ion batteries. To achieve this goal, one approach would be to replace the $LiPF_6$-based electrolytes which produce HF and precipitate LiF. However, there is currently no superior counterpart that provides a better compromise between conductivity, thermal stability, toxicity, corrosiveness and cost effectiveness.[12] An alternative approach is to limit the direct electrode-electrolyte contact by placing a barrier between them. Unlike the solid electrolyte interphase (SEI) on carbon-based anodes, the self-evolving surface layers on cathode particles do not provide protection during operation of the battery.[1] However, a barrier can be introduced artificially by applying a coating material to the cathode.[13,14] The pioneering work of Cho et al.[14] demonstrated that an Al_2O_3-coating on $LiCoO_2$ improves the capacity retention of Li-ion batteries. Numerous subsequent studies[15–24] have shown that Al_2O_3-coated cathodes exhibit improved properties. Many other coating materials have also been investigated such as phosphates,[15,22,25–27] carbonates,[28] hydroxides,[29] oxides (such as ZnO,[15–17,30,31] ZrO_2,[15–17,21,23,24,32] TiO_2,[21,23,32,33] MgO,[17,20,34–37] SiO_2,[23,24] Cr_2O_3,[38] Nb_2O_5,[16] Ta_2O_5,[16] SnO_2[20] and B_2O_3[21,23]) and fluorides (such as AlF_3,[13,15,17,39–41] CaF_2,[42] MgF_2[43] and LaF_3[43]). The oxides and fluorides have received the most attention, and we concentrate on binary oxides and fluorides as cathode coating candidates in this paper.

Although many cathode coating studies demonstrate improvements in capacity retention of the Li-ion batteries, the protection mechanisms are not completely understood.[25] One important protection mechanism called HF-scavenging has been suggested due to experiments that show the amount of dissolved redox-active metal-ion is proportional to the amount of HF in the electrolyte, and both decrease in presence of an HF-scavenging oxide coating.[18,23,44] Myung et al.[19] have confirmed that Al_2O_3 coatings react with HF and transform into AlF_3 via,

$$Al_2O_3 + 6HF \rightarrow 2AlF_3 + 3H_2O \quad (3)$$

Equation (3) is a typical HF-scavenging reaction. Metal oxides can serve as HF-scavenging coatings[15] but the extent

© 2014 WILEY-VCH Verlag GmbH & Co. KGaA, Weinheim

AMPEREX Ex. 1024
Page 1

of protection depends on the oxide.[23] Equation (3) shows that a fluoride layer can form on top of an HF-scavenging oxide coating as a product of the HF-scavenging reaction. This fluoride layer can provide an additional protection, forming a permanent physical barrier[15] that restricts penetration of HF through the oxide coating.

In addition to the protective chemical reactivity with the electrolyte, a coating material can also react with the active-Li in the battery, which may have undesired consequences. First, stable oxides or fluorides in a coating are expected to absorb Li mainly via conversion reactions with sluggish kinetics,[45,46] which can lead to capacity loss at high (dis)charge rates and/or an increase in cell polarization. Second, LiF is an undesired product of the electrolyte degradation (Equation (1)) due to its low permeability to Li-ions[8,9] and electrons,[10] and lithiation of metal fluoride layers may further contribute to LiF production and deteriorate the performance of the cathode.

Experimental efforts to discover improved cathode coatings have often followed a largely Edisonian approach of fabricating, cycling and disassembling Li-ion batteries. To accelerate this process, we propose a material design framework, screening the candidate set of materials on the basis of a target set of attributes. Several of our screens involve the thermodynamics of reactions of coating materials with HF and Li. However, thermodynamic screening of a great many prospective coating materials is hindered by the lack of experimental thermodynamic data of fluorides in thermochemical tables[47–49] or by the large uncertainties in the available data. Hence, we use density functional theory (DFT), a well-established first-principles method that has extensively aided understanding and improvement of electrodes and electrolytes for Li-ion batteries[50–59] to predict materials thermodynamics. We integrate DFT-based thermodynamics with a coating design framework and present a novel combinatorial approach to screen cathode coating candidates for Li-ion batteries. Materials screening based on descriptors calculated with first-principles methods, as we present in this work, has become a prominent approach to discovering new materials for various applications.[60]

The current understanding of cathode coatings has allowed us to construct the following three-part thermodynamic design framework: 1) HF-scavenging tendencies: Although several proposals exist for dissolution mechanisms of redox-active metal-ions from cathodes[11,61–63] the exact mechanism of how HF participates in dissolution reactions is not well-known. On the other hand, coating materials have already been observed to decrease the HF content of the electrolyte. Therefore, for batteries where HF-scavenging is a possible protection mechanism, a rational thermodynamic screening for HF-scavenging tendencies of oxide coatings can be done by ranking them with respect to the energetics of the scavenging reaction. 2) Cyclable-Li loss: Li-loss can take place into any component of the coating; i.e., an oxide coating itself, as well as a fluoride layer formed by HF-scavenging or a directly applied fluoride coating that aims at serving as a physical protection layer. Therefore, potential reaction of coatings with Li is not only important for screening the oxides but also important for the fluorides. In order to assess the interaction of Li with coatings both before and after their reaction with HF, we present DFT calculations of lithiation voltages and implement them in our design framework via the following design criterion: the lithiation voltage of a component of a coating (and subsequent layers that may form) should be lower than the (to-be-defined) discharge cutoff voltage of the cathode. This criterion ensures that it is always energetically more favorable for Li to react with the cathode phase rather than the components of the coating so that the coating does not tend to absorb cyclable-Li during cycling. 3) LiF-scavenging tendencies: LiF precipitates on the surface of the cathode particles due to electrolyte degradation reactions (Equation (1)). Compared to other organic and inorganic Li-based compounds precipitating on the electrodes, LiF has a very low room temperature Li diffusivity[8,9] and is a wide-bandgap insulator.[10] As a consequence, LiF increases the interface impedance[64] and is an undesired species on the surface of a cathode particle. These features of LiF motivate us to seek ways to scavenge LiF as a part of our design framework. In analogy to HF-scavenging, LiF-scavenging tendencies of coatings can be ranked based on the energetics of LiF-scavenging reactions.

Here, we analyze a wide range of s-, p- and d-block binary metal oxides and fluorides as cathode coating materials within the DFT-based thermodynamic design framework outlined above according to the HF-scavenging mechanism suggested in experiments. We calculate the enthalpies of HF-scavenging reactions and lithiation voltages of binary metal oxides and fluorides, and compare our results to the available experimental data. We incorporate the calculated enthalpies of HF-scavenging reactions, volumetric and gravimetric HF-scavenging capacities, and lithiation voltages into a combinatorial design chart which allows simultaneous comparison of all these properties. On the basis of this comparison, we find that the enhancements in capacity retention provided by experimentally tested coatings such as Al_2O_3, ZrO_2, TiO_2 and MgO are consistent with calculated design attributes. In addition, we predict promising and as yet unexplored or underexplored cathode coatings such as trivalent transition metal oxides (e.g., Sc_2O_3, Ti_2O_3, V_2O_3, Cr_2O_3, Mn_2O_3 and Y_2O_3) for batteries with HF-bearing electrolytes. Finally, we present the enthalpies of LiF-scavenging reactions and show that LiF-scavenging could be another protection mechanism that operates in addition to HF-scavenging.

2. Methods

2.1. First-Principles Calculations

All DFT calculations were carried out using the Vienna Ab initio simulation package (VASP)[65–68] with projector augmented wave (PAW) potentials[69] and the Perdew-Burke-Ernzerhof (PBE) formulation[70,71] of the generalized gradient approximation (GGA) for the exchange-correlation functional. For all compounds, we use a cutoff energy of 520 eV for the plane-wave basis set and k-point meshes with a nominal density of 8,000 k-points per reciprocal atom, except for molecules for which utilizing only the Γ-point is sufficient. To compare with DFT calculations, we performed DFT+U calculations with the rotationally invariant formulation of Dudarev et al.[72] for HF-scavenging reactions of compounds of Fe, Co, Mn, Cr, Ni, V and Cu. The U values reported by Wang et al.[73] were applied to oxides and fluorides of the mentioned 3d-metals in DFT+U calculations.

© 2014 WILEY-VCH Verlag GmbH & Co. KGaA, Weinheim

AMPEREX Ex. 1024
Page 2
16146840, 2014, 17, Downloaded from https://onlinelibrary.wiley.com/doi/10.1002/aenm.201400690 by Jennifer Babbitt , Wiley Online Library on [05/05/2023]. See the Terms and Conditions (https://onlinelibrary.wiley.com/terms-and-conditions) on Wiley Online Library for rules of use; OA articles are governed by the applicable Creative Commons License

16146840, 2014, 17, Downloaded from https://onlinelibrary.wiley.com/doi/10.1002/aenm.201400690 by Jennifer Babbitt , Wiley Online Library on [05/05/2023]. See the Terms and Conditions (https://onlinelibrary.wiley.com/terms-and-conditions) on Wiley Online Library for rules of use; OA articles are governed by the applicable Creative Commons License

Structures were fully relaxed with respect to all internal and external degrees of freedom of the cell, and total energies were evaluated in a final static run. All crystal structures are from the Inorganic Crystal Structure Database (ICSD).[74] The calculations were performed using the computation framework provided by the open quantum materials database (OQMD).[75,76] For all reactions considered in this study, the enthalpies of compounds at $T = 0$ K were approximated by DFT total energies (PV contributions were neglected). Numerical values of calculated properties are available as Supporting Information.

2.2. Selection of Experimental Thermochemical Data and Method of Error Analysis

Experimental thermochemical data were mostly collected from the tables of JANAF[47] and Kubaschewski,[48] while for data not available in these tables, we refer to Thermochemical Data of Pure Substances[49] or other cited literature. To calculate experimental reaction enthalpies, we used experimental formation enthalpies (ΔH_f^{exp}). When the enthalpy of a reaction involving multiple compounds (such as HF-scavenging and lithiation reactions) is calculated using ΔH_f^{exp} of each compound in that reaction, the uncertainties in ΔH_f^{exp} values propagate. Hence, when available, we used the reported uncertainties (u_i) in ΔH_f^{exp} of compounds to calculate the experimental combined standard uncertainty (CSU) of a reaction enthalpy by $\mathrm{CSU} = \left(\sum_i c_i^2 u_i^2\right)^{1/2}$, where c_i is the coefficient compound i takes in the reaction. We calculated the CSU of an experimental reaction enthalpy if the formation enthalpies of all compounds in the reaction have a corresponding u_i reported in thermochemical tables. The mean absolute error (MAE) for a set of n number of calculated reaction enthalpies is defined as $\mathrm{MAE} = n^{-1}\sum_{j=1}^{n}\left|\Delta H_j^{exp} - \Delta H_j^{calc}\right|$, where ΔH_j^{exp} and ΔH_j^{calc} are experimental and calculated enthalpies of the jth reaction, respectively. We should note that since the DFT enthalpies correspond to 0 K, they should be compared with the experimental enthalpies at 0 K when possible. For many compounds, thermochemical tables such as JANAF[47] list ΔH_f^{exp} values at 0 K, obtained by systematically extrapolating the finite temperature ΔH_f^{exp} values to 0 K via integration of experimental heat capacities. Therefore, we calculated the experimental enthalpy of a reaction using the ΔH_f^{exp} reported at 0 K in such tables, but only if that exists for all compounds in the reaction. Otherwise, if ΔH_f^{exp} at 0 K is not known for any of the compounds, we used ΔH_f^{exp} at 298 K for all compounds in the reaction. We estimated the difference between 298 K and 0 K reaction energies using several HF-scavenging reactions (see the Supporting Information) to be around 11 meV on average. Since this energy difference is much smaller than the average experimental uncertainty of 55 meV (**Table 1**), DFT data corresponding to 0 K and experimental data at 298 K can be safely compared.

3. Results and Discussion

3.1. HF-Scavenging by Binary Oxides: DFT vs Experiment

For metal oxide coatings, the HF-scavenging reaction per mole of HF can be written in the generic form,

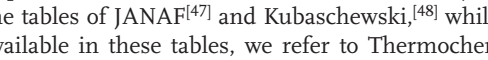

$$M_xO_{1/2} + HF \rightarrow M_xF + 1/2H_2O \quad (4)$$

where we adapt the forms $M_xO_{1/2}$ and M_xF to represent the oxide and fluoride of M (with a certain oxidation state), respectively, so as to simplify the HF-scavenging reaction by having a single stoichiometry variable (x) that can describe both phases of M. We want to rank metal oxides by the enthalpy of this reaction (ΔH_{s-HF}) which reflects the HF-scavenging tendency of the oxide $M_xO_{1/2}$. The DFT enthalpy of this reaction (ΔH_{s-HF}^{DFT}) at zero temperature and pressure can be calculated using DFT total energies (E) as,

$$\Delta H_{s-HF}^{DFT}\left[M_xO_{1/2}\right] = E_{M_xF}^{DFT} + 1/2E_{H_2O}^{DFT} - E_{M_xO_{1/2}}^{DFT} - E_{HF}^{DFT} \quad (5)$$

The corresponding experimental enthalpy (ΔH_{s-HF}^{exp}) can be calculated using ΔH_f^{exp} of each compound as,

$$\Delta H_{s-HF}^{exp}\left[M_xO_{1/2}\right] = \Delta H_{f,M_xF}^{exp} + 1/2\Delta H_{f,H_2O}^{exp} - \Delta H_{f,M_xO_{1/2}}^{exp} - \Delta H_{f,HF}^{exp} \quad (6)$$

In Equation (5), we see that the difference between ΔH_{s-HF}^{DFT} of two different coatings depends only on the energies of $M_xO_{1/2}$ and M_xF, as is evident from the reaction stoichiometry of HF and H_2O being fixed (as 1:½) for all reactions written in the form of Equation (4). Thus, the relative ranking of coatings with respect to ΔH_{s-HF}^{DFT} is independent of the energetic contribution of HF and H_2O (i.e., $1/2E_{H_2O}^{DFT} - E_{HF}^{DFT}$) in Equation (5), and we can simply treat HF and H_2O as isolated molecules. Nevertheless, to separate any DFT errors related to molecules from other sources of errors, a correction for $1/2E_{H_2O}^{DFT} - E_{HF}^{DFT}$ can be found

Table 1. The mean combined standard uncertainty (mean-CSU) in experimental values and mean absolute error (MAE) of DFT values relative to experiment for HF-scavenging enthalpies and voltages of oxides and fluorides.

Compounds[b)]	mean-CSU[a)]			MAE		
	ΔH_{s-HF} [eV HF^{-1}]	$\bar{V}_{M_xO_{1/2}}$ [V]	$\bar{V}_{M_xF}$ [V]	ΔH_{s-HF} [eV HF^{-1}]	$\bar{V}_{M_xO_{1/2}}$ [V]	$\bar{V}_{M_xF}$ [V]
Simple	0.021	0.018	0.017	0.029	0.027	0.031
p- and d-block	0.070	0.014	0.070	0.157	0.160	0.277
All	0.055	0.015	0.053	0.125	0.128	0.219

[a)]There are 35 oxide/fluoride pairs with experimental uncertainties available and CSU values can be calculated for their reactions; [b)]"Simple" denotes compounds of alkali and alkaline earths, Al and Zn. "p- and d-block" denotes compounds of p- and d-block metals/semi-metals, and Be is also included in this set.

© 2014 WILEY-VCH Verlag GmbH & Co. KGaA, Weinheim

AMPEREX Ex. 1024
Page 3

by fitting the DFT enthalpies of simple metal compound reactions, to the experimental counterparts (ΔH^{exp}_{s-HF}).[73,77] As shown in **Figure 1**, the agreement of uncorrected ΔH^{DFT}_{s-HF} with ΔH^{exp}_{s-HF} for the simple metal compound reactions is already extremely good, and apparently no significant correction to DFT energies of HF and ½ H_2O is required in ΔH^{DFT}_{s-HF}. This implies even if there are any errors associated with DFT description of molecular HF and H_2O, they cancel out.

Searching the ICSD for pairs of s-, p- and d-block binary metal oxides and fluorides that satisfy the form of the HF-scavenging reaction given in Equation (4), we found 81 different reactions. However, in this set of 81 reactions, 40 reactions have either an oxide or fluoride with an experimental formation enthalpy not available in thermochemical tables; thus, ΔH^{exp}_{s-HF} of these reactions cannot be evaluated using experimental data. The remaining reactions have ΔH^{exp}_{s-HF} available for both oxide and fluoride, and we compare the corresponding ΔH^{exp}_{s-HF} and ΔH^{DFT}_{s-HF} values in Figure 1 (simple metal compounds) and **Figure 2** (p- and d-block compounds). We further list the mean-CSU and MAE values in Table 1.

While it is straightforward to calculate the experimental reaction enthalpies using ΔH^{exp}_f, one has to consider the propagation of uncertainties when ΔH^{exp}_f values are linearly combined, and carefully compare the magnitude of the CSU to the calculated enthalpy. We, therefore, show the CSU values of ΔH^{exp}_{s-HF} (as error-bars) in Figures 1 and 2. Experimental uncertainties in ΔH^{exp}_f of simple metal compounds are generally on the order of ≈0.01 – 0.02 eV, which leads to the relatively small error-bars in Figure 1. Their mean-CSU is 0.021 eV HF^{-1} as

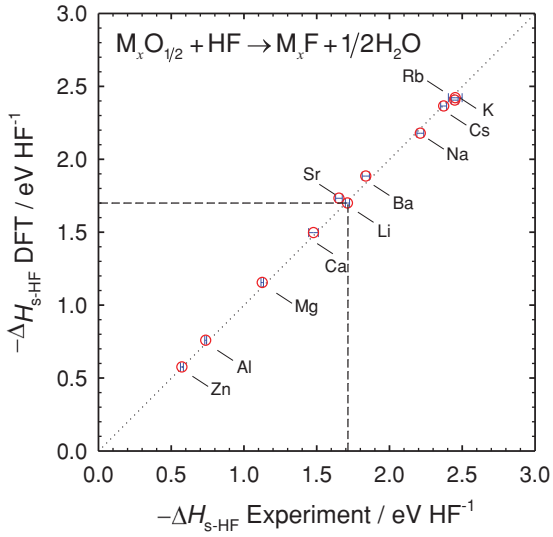

Figure 1. Comparison of HF-scavenging reaction enthalpies of simple metal oxides ($M_xO_{1/2}$ where M is an alkali or alkaline-earth metal, Al or Zn) calculated by DFT (Equation (5)) with the experimental enthalpies calculated using available thermochemical data (Equation (6)). Using DFT energies for HF and H_2O results in an excellent agreement with experiment, obviating the need for energy corrections for molecules.[73,77] The error-bars show combined standard uncertainties (CSU) in experimental values. The dashed-lines show the enthalpy limit $\Delta H_{s-HF}[Li_2O]$, below which voltage of M_xF is always higher than the corresponding $M_xO_{1/2}$. The dotted-line represents perfect agreement with experiment.

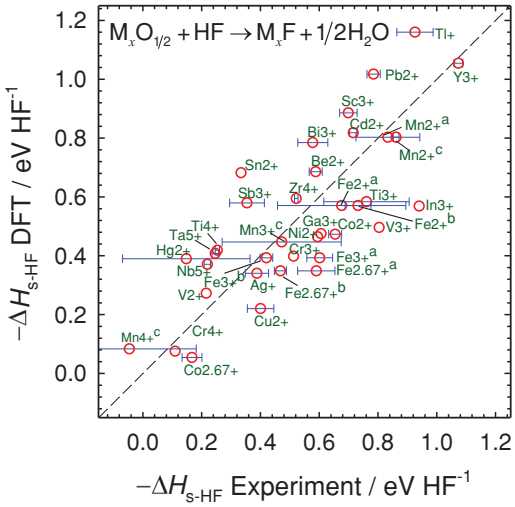

Figure 2. Comparison of HF-scavenging reaction enthalpies of p- and d-block metal oxides calculated by DFT (Equation (5)) with the experimental enthalpies calculated using available thermochemical data (Equation (6)). The error-bars show combined standard uncertainties (CSU) in experimental values. The superscript "a" denotes values listed in thermochemical tables, "b" denotes ref. [78,79] and "c" denotes ref. [80,81] M2.67+ corresponds to M_3O_4 reacting with HF to produce MF_2 and MF_3. BeO is also included in this plot. The dashed-line represents perfect agreement with experiment.

shown in Table 1. On the other hand, ΔH^{exp}_{s-HF} of most of the p- and d-block fluorides bear large uncertainties ranging from ±0.05 to ±0.4 eV. Consequently, the CSUs in experimental reaction enthalpies of p- and d-block compounds in Figure 2 are much higher than that of simple metal compounds (as high as ≈0.30 eV HF^{-1} for several reactions). Relative-CSU values (i.e., CSU/$|\Delta H|$) range from ≈5% to over 100% in experimental ΔH^{exp}_{s-HF} of p- and d-block compounds. Furthermore, there are large discrepancies between ΔH^{exp}_f reports in thermochemical tables and more recent literature, ranging from ≈0.1 eV (e.g., FeF_2[78] and MnF_2[80]) to ≈0.5 eV (e.g., FeF_3[77]). Consequently, a straightforward validation of ΔH^{DFT}_{s-HF} by comparing to ΔH^{exp}_{s-HF} for p- and d-block metal compounds is hindered by the large uncertainties and discrepancies in experimental data, unlike the s-block compounds. Nevertheless, the difference between the mean-CSU of 0.070 eV HF^{-1} and the corresponding DFT MAE of 0.157 eV HF^{-1} is relatively small, which implies DFT calculations can provide an acceptable level of accuracy in enthalpies of HF-scavenging reactions of p- and d-block metal oxides. Thus, a DFT treatment of Equation (4) can help systematically study the thermodynamics in p- and d-block metal oxide HF-scavenging reactions.

For several d-block metal compounds, we further tested the calculated enthalpies of HF-scavenging reactions involving Fe, Co, Mn, Cr, Ni, V and Cu with the DFT+U method as well. Although applying U slightly decreases the MAE from 0.157 to 0.149 eV HF^{-1}, the decrease is an order of magnitude smaller than the mean-CSU of 0.070 eV HF^{-1} in experiments. So, the use of DFT+U for these reaction enthalpies does not provide a significantly more accurate description than DFT. Consequently, we report and use mainly the results of the DFT calculations in this work.

© 2014 WILEY-VCH Verlag GmbH & Co. KGaA, Weinheim

AMPEREX Ex. 1024
Page 4
16146840, 2014, 17, Downloaded from https://onlinelibrary.wiley.com/doi/10.1002/aenm.201400690 by Jennifer Babbitt , Wiley Online Library on [05/05/2023]. See the Terms and Conditions (https://onlinelibrary.wiley.com/terms-and-conditions) on Wiley Online Library for rules of use; OA articles are governed by the applicable Creative Commons License

16146840, 2014, 17, Downloaded from https://onlinelibrary.wiley.com/doi/10.1002/aenm.201400690 by Jennifer Babbitt , Wiley Online Library on [05/05/2023]. See the Terms and Conditions (https://onlinelibrary.wiley.com/terms-and-conditions) on Wiley Online Library for rules of use; OA articles are governed by the applicable Creative Commons License

3.2. Lithiation Reactions of Protective Layers: DFT vs Experiment

Lithium can be trapped in the protective layers (both oxide and fluoride) during cycling. In this section, we evaluate the average lithiation voltages of binary oxides and fluorides via DFT calculations and compare them to the voltages calculated from experimental data. For oxides and fluorides, overall conversion reactions can be written as,

$$M_xO_{1/2} + Li \rightarrow xM + 1/2Li_2O \tag{7}$$

$$M_xF + Li \rightarrow xM + LiF \tag{8}$$

respectively. When approximated at $T = 0$ K, Gibbs free energy of the lithiation reactions in Equation (7) and (8) reduce to their enthalpies, which can be evaluated via DFT total energies as,

$$\Delta H_{Li}^{DFT}\left[M_xO_{1/2}\right] = xE_M^{DFT} + 1/2E_{Li_2O}^{DFT} - E_{M_xO_{1/2}}^{DFT} - E_{Li}^{DFT} \tag{9}$$

$$\Delta H_{Li}^{DFT}\left[M_xF\right] = xE_M^{DFT} + E_{LiF}^{DFT} - E_{M_xF}^{DFT} - E_{Li}^{DFT} \tag{10}$$

respectively. The experimental counterparts of these enthalpies can be calculated from the formation enthalpies as,

$$\Delta H_{Li}^{exp}\left[M_xO_{1/2}\right] = 1/2\Delta H_{f,Li_2O}^{exp} - \Delta H_{f,M_xO_{1/2}}^{exp} \tag{11}$$

$$\Delta H_{Li}^{exp}\left[M_xF\right] = \Delta H_{f,LiF}^{exp} - \Delta H_{f,M_xF}^{exp} \tag{12}$$

With the enthalpies defined above, the average DFT or experimental voltage upon transfer of n electrons can be calculated as,

$$V_i \approx -\Delta H_{Li}\left[i\right]/ne \tag{13}$$

for the conversion reaction of compound i. Since intermediate reaction steps or direct lithium insertion into phases are not considered in Equation (7) and (8), the calculated voltages correspond to average voltages (vs Li metal) of conversion of $M_xO_{1/2}$ and M_xF, which we denote as $V_{M_xO_{1/2}}$ and V_{M_xF}, respectively. Calculated DFT voltages of oxides and fluorides are compared to the experimental counterparts calculated from ΔH_f^{exp} available in thermochemical tables[47–49] in **Figure 3**.

The accuracy of DFT lithiation voltages can be assessed by comparing the MAE in DFT voltages to the mean-CSU in experimental counterparts listed in Table 1. Similar to the HF-scavenging reactions, DFT voltages are also highly accurate for simple metal compounds (both for oxides and fluorides) since their MAE is small and similar to the mean-CSU of experimental voltages. On the other hand, while the mean-CSU in voltages of p- and d-block metal oxides is still small (0.014 V), that of corresponding fluorides is large (0.070 V) due to large uncertainties in ΔH_f^{exp} of fluorides. The difference between DFT MAE and mean-CSU in experimental values, however, is around 0.15–0.20 V for both oxides and fluorides. Therefore, we conclude that current DFT calculations for p- and d-block metal oxides and fluorides provide an acceptable level of lithiation voltage accuracy on the order of approximately ±0.20 V.

From Equation (9)–(13), one can show that a simple relation exists between the lithiation voltages and the HF-scavenging enthalpies:

$$V_{M_xO_{1/2}} = V_{M_xF} - e^{-1}\left(\Delta H_{s-HF}\left[M_xO_{1/2}\right] - \Delta H_{s-HF}\left[Li_2O\right]\right) \tag{14}$$

This relation tells us for a given metal M in a certain oxidation state, $V_{M_xO_{1/2}}$ becomes larger than V_{M_xF} only if $\Delta H_{s-HF}\left[M_xO_{1/2}\right]$ of the HF-scavenging reaction is more negative than that of Li, $\Delta H_{s-HF}\left[Li_2O\right]$. Hence, except for a few s-block metals; namely, M = Rb, Cs, K, Sr, Na and Ba (see Figure 1), V_{M_xF} of a binary fluoride is greater than $V_{M_xO_{1/2}}$ of its corresponding binary oxide. This trend is expected from the larger electronegativity of fluorine compared to oxygen,[82] and it means that fluorides often have a higher tendency to react with Li than oxides. As seen in **Figure 4**, the difference between V_{M_xF} and $V_{M_xO_{1/2}}$ values varies between approximately 1.0 and 1.5 V. In Figure 4, among the 81 pairs of $M_xO_{1/2}$ and M_xF, coatings that are out of the region enclosed by the dashed line (which is an arbitrary cutoff voltage of 3.0 V) will potentially absorb Li during discharge.

3.3. A Combinatorial Design Approach for HF–Scavenger Coatings

3.3.1. The Design Chart for Cathode Coatings

The HF-scavenging tendencies and lithiation voltages are the two principal thermodynamic parameters we have discussed, the former being important for screening oxides and the latter being important for screening both oxides and fluorides. We can also define two additional design attributes; namely, the volumetric HF-scavenging capacity (Ω_V) and the gravimetric HF-scavenging capacity (Ω_G) as the number of moles of HF the oxide coating can scavenge per unit volume and per gram, respectively. A high Ω_V is desired because it is inversely related to the volume of the Li^+ diffusion barrier that is placed between the cathode and the electrolyte. The gravimetric counterpart Ω_G should also be high to design lighter cells with higher capacities; i.e., it directly affects the specific capacity and energy density of the battery.

We combine these four properties we want to optimize in a design chart in **Figure 5**, where HF-scavenging tendencies of oxides ($-\Delta H_{s-HF}$) and lithiation voltages of fluoride layers forming as a product of HF-scavenging (or coated directly) are compared as a function of Ω_V and Ω_G. Upon discharge, Li will thermodynamically prefer to react with the coating component that has the higher voltage. Hence, we select V_{M_xF} instead of $V_{M_xO_{1/2}}$ as a design parameter in Figure 5 because $V_{M_xF} > V_{M_xO_{1/2}}$ for almost all cases as we have already shown in Figure 4 via analyzing Equation (14). The only exception to this are a few s-block metal compounds but this is not critical, because their oxides and fluorides both have very small conversion voltages in Figure 4 (below ≈1.0 V) which would presumably not be reached upon discharging a typical Li-ion battery (a typical discharge cutoff voltage is often around 3.0 V[18–20,28,34]). Figure 5 consists of four different plots brought together. For each metal oxide/fluoride pair that appears in the 81 HF-scavenging reactions we devised, there is a unique point in each panel that can be connected by drawing horizontal and vertical lines. These

© 2014 WILEY-VCH Verlag GmbH & Co. KGaA, Weinheim

AMPEREX Ex. 1024
Page 5

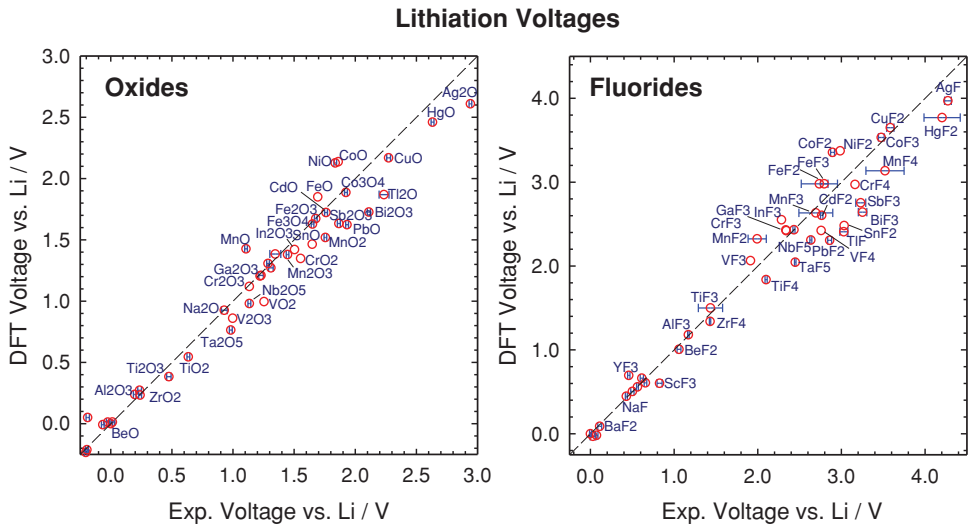

Figure 3. Calculated average voltages for oxides and fluorides versus voltages estimated from experimental formation enthalpies. Voltages for oxides and fluorides correspond to conversion reactions $M_xO_{1/2} + Li \rightarrow xM + 1/2Li_2O$ and $M_xF + Li \rightarrow xM + LiF$, respectively, and they are calculated as described in Equations (9–13). The error-bars show combined standard uncertainties (CSU) in experimental values.

lines combine to form property rectangles. For example, the property rectangle sketched for Al^{3+} in Figure 5 encloses coatings inferior to the oxide/fluoride of Al^{3+}. For materials that are close in every panel such as Al^{3+} and Mg^{2+}, we expect a similar coating performance in terms of the metrics in Figure 5.

3.3.2. Constraints on the Design Parameters: the Criteria of Screening

For the HF-scavenging tendencies of oxides, we put forward a simple criterion; i.e., the larger $-\Delta H_{s-HF}$, the more effective the coating will be at scavenging HF. However, there should also be a lower limit for $-\Delta H_{s-HF}$ that ensures the preferential reaction of HF with the coating in the presence of the cathode, but it requires knowing the enthalpy of reaction of HF with the cathode. Therefore, to estimate a lower limit for $-\Delta H_{s-HF}$, we adopt simple HF-attack reactions analogous to Equation (4) for common cathode materials listed in **Table 2**. These reactions are not meant to be prescriptive of the actual dissolution mechanisms that would take place via solvated ions (for which Benedek and van de Walle introduced a hybrid computational method[61]). Nevertheless, reactions in Table 2 provide us with estimates for the magnitudes of the enthalpies of the HF-attack reactions for typical cathode materials in a form consistent with Equation (4) so that we can compare their $-\Delta H_{s-HF}$ to that of the coatings. We see that the reaction enthalpies in Table 2 are around −0.3 eV HF^{-1} for almost all cathode materials listed except for $LiMnO_2$ (which means fewer coatings can provide preferential HF-scavenging for $LiMnO_2$ cathodes compared to other cathodes listed in Table 2). Thus, since we are searching for oxide coatings that preferentially react with HF in presence of cathode particles, we constrain $-\Delta H_{s-HF}$ to have a lower bound of 0.3 eV HF^{-1}. For example, Al_2O_3 coatings have been shown to preferentially react with HF to form AlF_3,[19,86] and the HF-scavenging tendency $-\Delta H_{s-HF}$ = 0.76 eV HF^{-1} of Al_2O_3 is more than twice as large as 0.3 eV HF^{-1}. To determine an upper bound is not as straightforward because the HF-scavenging tendency is related to the general reactivity of a compound. For example, HF-scavenging tendency of alkaline-earth oxides increases in the order MgO < CaO < SrO < BaO as seen in Figure 1, which is identical to the pattern followed by the surface reactivity of these materials.[87] Thus, very large $-\Delta H_{s-HF}$ values suggest an extremely reactive coating, which may show a tendency to react also with materials present in the cell, other than HF. However, we cannot quantify a precise value of $-\Delta H_{s-HF}$ that would indicate an "excess reactivity." Upon screening, we select $-\Delta H_{s-HF}$ of CaO as an upper limit.

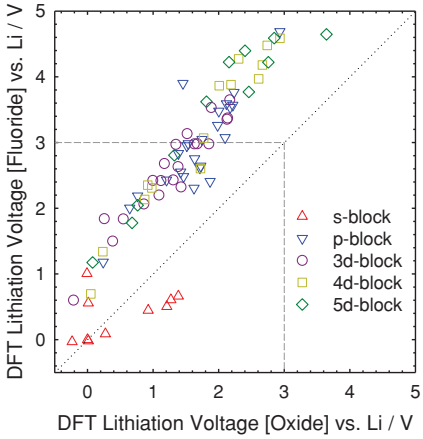

Figure 4. DFT average lithiation voltages of s-, p- and d-block metal oxides and fluorides, via the conversion reactions of the form $M_xO_{1/2} + Li \rightarrow xM + 1/2Li_2O$ and $M_xF + Li \rightarrow xM + LiF$, respectively. The dashed-line is an arbitrary discharge cutoff voltage (i.e., the lowest voltage attained during the discharge) of 3.0 V for a sample cathode to be coated. If a prospective coating for this sample cathode has a lithiation voltage lower than the discharge cutoff of the cathode (i.e., the components of the coating lie in the window enclosed by the dashed-lines), the coating will not tend to absorb lithium.

© 2014 WILEY-VCH Verlag GmbH & Co. KGaA, Weinheim

AMPEREX Ex. 1024
Page 6
16146840, 2014, 17, Downloaded from https://onlinelibrary.wiley.com/doi/10.1002/aenm.201400690 by Jennifer Babbit , Wiley Online Library on [05/05/2023]. See the Terms and Conditions (https://onlinelibrary.wiley.com/terms-and-conditions) on Wiley Online Library for rules of use; OA articles are governed by the applicable Creative Commons License

ADVANCED ENERGY MATERIALS
www.advenergymat.de

16146840, 2014, 17, Downloaded from https://onlinelibrary.wiley.com/doi/10.1002/aenm.201400690 by Jennifer Babbitt , Wiley Online Library on [05/05/2023]. See the Terms and Conditions (https://onlinelibrary.wiley.com/terms-and-conditions) on Wiley Online Library for rules of use; OA articles are governed by the applicable Creative Commons License

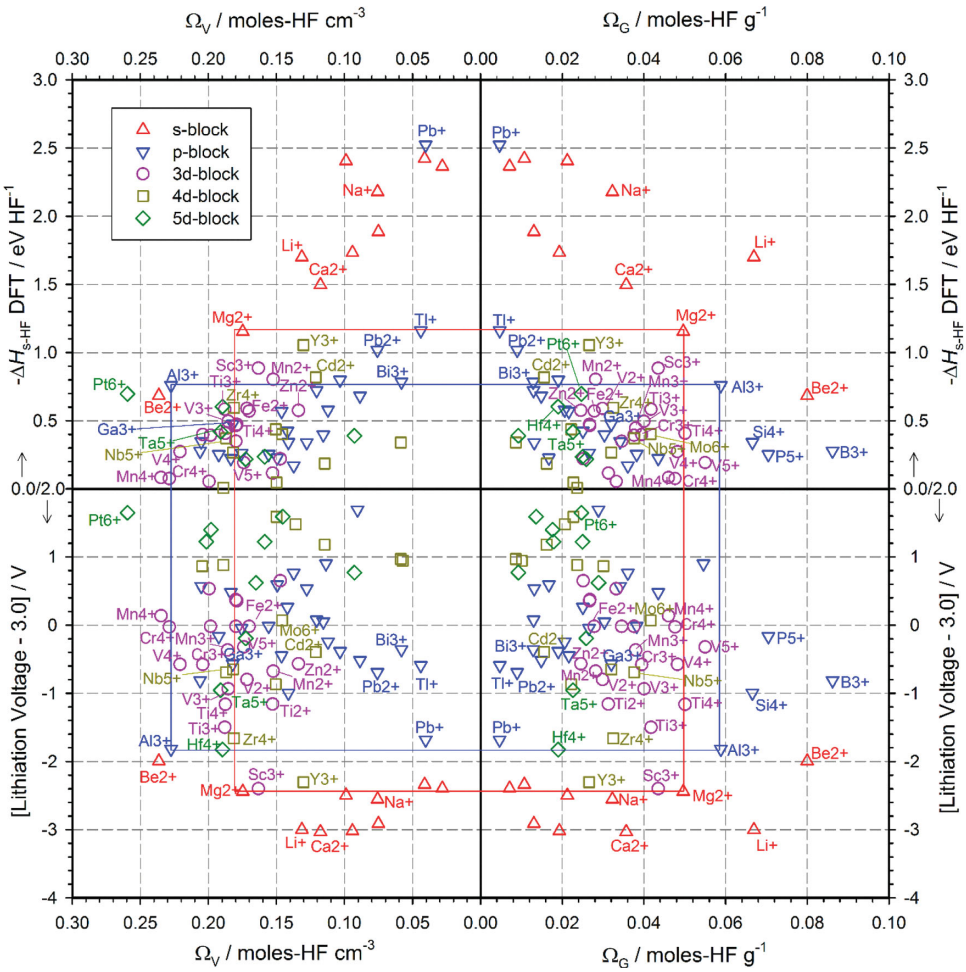

Figure 5. The design chart for comparing HF-scavenging tendencies of oxides ($-\Delta H_{s-HF}$), lithiation voltages of their corresponding fluorides relative to an arbitrary discharge cutoff of 3.0 V ($V_{M_xF} - 3.0$), Ω_V and Ω_G of 81 metal-oxide coating candidates for Li-ion battery cathodes. Compounds are labeled with their cations for simplicity. Sample property rectangles are drawn for Al^{3+} and Mg^{2+}. Such a rectangle for a material shows that it is thermodynamically a better coating than materials that remain inside.

To avoid active-Li loss into a coating, lithiation voltages of the coating components should be lower than the lowest voltage attained during the discharge of the battery. For Li-ion batteries, a typical discharge cutoff is around 3.0 V, and we include this value as an illustrative limit in the form $V_{M_xF} - 3.0$ in the lower panels of Figure 5. A coating with a negative V_{M_xF} value satisfies this criterion. On the other hand, there is no apparent reason to demand the coating voltage to be as low as possible, so we do not adopt a lower voltage limit as a criterion.

3.3.3. Validation of the Design Framework

Capacity retention attained in the presence of coatings tested under identical experimental conditions can be compared with the design chart in Figure 5 to see whether the experimental trends are captured with the current thermodynamic design approach. For example, the ranking of capacity retention in the presence of coatings tested by Kim et al.[23] is ZrO_2 > Al_2O_3 > TiO_2 > B_2O_3 > SiO_2 > bare (uncoated $LiCoO_2$). Compared to other materials they tested, our calculations show both Al_2O_3 and ZrO_2 have higher HF-scavenging tendencies with good scavenging capacities, and their fluorides AlF_3 and ZrF_4 have low lithiation voltages. Therefore, Al_2O_3 and ZrO_2 are expected to be good coatings, in agreement with findings of Kim et al. Our screen predicts SiO_2 and B_2O_3 to be inferior to TiO_2 due to lower HF-scavenging tendencies and higher lithiation voltages. This result is also consistent with observations. However, the significant performance drop with SiO_2 and B_2O_3 coatings observed by Kim et al. hints at the presence of an additional drawback of these HF-scavenging coatings; i.e., SiF_4 and BF_3 are not stable solids at room temperature. The HF-scavenging reactions of SiO_2 and B_2O_3, therefore, cannot produce protective fluoride layers, and consumption of the oxide by HF eventually exposes $LiCoO_2$ particles to HF during cycling. As a further test of this hypothesis, a P_2O_5 coating also has an HF-scavenging product (PF_5) that does not form a solid phase around room temperature. The findings of Cho and co-workers[88] confirm our hypothesis by showing that P_2O_5-coating actually deteriorates the capacity retention of $LiCoO_2$, the excessive capacity

 © 2014 WILEY-VCH Verlag GmbH & Co. KGaA, Weinheim

AMPEREX Ex. 1024
Page 7

Table 2. Enthalpies of reactions of common cathode materials with HF. For all cathodes, we assumed a reaction form analogous to Equation (4). Products of the reactions are determined via the grand canonical linear programming (GCLP) method[55,83–85] as the ground state phases at the given composition in the corresponding chemical space.

Reaction	Enthalpy [eV HF^{-1}]
$1/4\ LiCoO_2 + HF \rightarrow 1/4\ LiCoF_4 + 1/2\ H_2O$	–0.32
$1/4\ LiNiO_2 + HF \rightarrow 1/4\ NiF_3 + 1/4\ LiF + 1/2\ H_2O$	–0.32
$1/8\ LiFePO_4 + HF \rightarrow 1/8\ FeF_2 + 1/8\ LiPF_6 + 1/2\ H_2O$	–0.28
$1/8\ LiMn_2O_4 + HF \rightarrow 1/8\ MnF_4 + 1/8\ LiMnF_4 + 1/2\ H_2O$	–0.29
$1/4\ LiMnO_2 + HF \rightarrow 1/4\ LiMnF_4 + 1/2\ H_2O$	–0.65

loss likely being a consequence of PF_5 replenishing the electrolyte with HF via Equation (2). Thus, we conclude that HF-scavenging can provide an effective protection mainly when the oxide coating can form a stable fluoride phase, and we take this into account upon screening.

With a Li-Co-Ni-Mn-O based cathode, Myung et al.[16] showed the following coatings can be ranked by the capacity retention they provide as Al_2O_3 > ZnO > Ta_2O_5 > ZrO_2 ≈ Nb_2O_5 > Bare, but this time the differences between coatings are not as pronounced as in the work of Kim et al.[23] This ranking of coatings is consistent with our calculations of HF-scavenging tendencies (except that we predict ZrO_2 to be better than Ta_2O_5.) In further support of our hypothesis of stable fluoride formation for extended protection, Myung et al. also suggested that the lower electrochemical performance of Nb_2O_5 and Ta_2O_5 coated cathodes results from NbF_5 and TaF_5 having low melting points (<100 °C). These low melting points imply that the produced fluoride layers are at higher homologous temperatures, and hence more susceptible to temperature-induced failure, near operating temperatures. In contrast to Myung et al., ZrO_2 is even better than Al_2O_3 on $LiCoO_2$ in ref. [23] This suggests the performances of coatings with similar attributes in Figure 5 (such as Al_2O_3 and ZrO_2) may strongly depend on additional factors such as the cathode material, coating morphology, thickness or fabrication method, etc. However, the overall agreement with the experimental trends indicates that the criteria we employ in our framework constitute a valid set of measures for screening performances of metal oxides as cathode coating materials.

3.3.4. Screening Materials to Find Promising Coating Candidates

Among the set of 81 candidates, 40 materials passed the preferential HF-scavenging and discharge cutoff voltage screens. From this set, we further eliminate high HF-scavenging tendency s-block oxides and low melting point fluorides (as explained in previous section) and obtain 27 HF-scavenger coating candidates shown in **Figure 6**. In this figure, to compare HF-scavenging capacities (Ω_V and Ω_G) of these compounds on a common scale, Ω_V and Ω_G are normalized via dividing by their largest values in this set (i.e., that of BeO). We also provide average normalized capacities that assume Ω_V and Ω_G are equally important. While materials that are known to be effective coatings (e.g., Al_2O_3, MgO, TiO_2 and ZrO_2) are already identified by our screening approach, several new candidates are also predicted in Figure 6. In this section, we discuss the properties of these promising coatings along with the already tested ones.

In agreement with its high protection performance confirmed in many experiments,[15–23] Al_2O_3 has an exceptionally good combination of attributes in Figure 5, not only among the p-block compounds but also among the entire set of compounds we consider. There is no other binary oxide in Figure 5 that simultaneously provides higher $-\Delta H_{s-HF}$, Ω_V and Ω_G than Al_2O_3. MgO and BeO are very close to Al_2O_3 and have high Ω_V and Ω_G, but BeO has an obvious drawback in battery manufacture due to toxicity concerns. Other s-block metal oxides provide the largest $-\Delta H_{s-HF}$ values and lowest voltages in Figure 5 with scavenging capacities considerably lower than Al_2O_3 or MgO. The performances of s-block compounds are likely to be hampered by low e- and/or Li^+ conductivities they or their HF-scavenging products (such as the undesired LiF in case of Li_2O) possibly have, while their reactivities may also impede their performance. Although it has lower Ω_V and Ω_G values than Al_2O_3, Ga_2O_3 is the only other p-block compound with an acceptable combination of attributes.

The most remarkable feature of transition metal oxide coatings is that in every panel of Figure 5, they occupy the region between Al_2O_3/MgO, and the cluster of p-block compounds close to the center of the plot. Several 3d-block compounds, and mostly the trivalent 3d-metal oxides, exhibit HF-scavenging tendencies and capacities much closer to Al_2O_3 than the rest of the p- or d-block compounds as shown in Figure 5 and 6. Sc_2O_3 is a prominent one among these, very close to Al_2O_3 and MgO in terms of all parameters. The rest of these viable coating candidates are Ti_2O_3, V_2O_3, Cr_2O_3, Mn_2O_3 and TiO_2. Among these, TiO_2[21,23,32,33] and Cr_2O_3[38] have already been reported to provide acceptable levels of protection. ZrO_2 and Y_2O_3 stand out among the 4d-block compounds. ZrO_2 has attracted significant attention as a cathode coating,[15–17,21,23,24,32] while we could find only a single study[89] regarding Y_2O_3. HfO_2 is a reasonable candidate from the 5d-block but its drawback is only a relatively small Ω_G.

3.4. LiF-Scavenging by Binary Fluorides

A concept we have introduced is scavenging the LiF precipitate from the cathode surface. LiF is a wide-bandgap material and has low Li^+ diffusivity. Fluorides, whether applied directly as coatings or produced by HF-scavenging reactions, can serve as LiF-scavengers if they react with LiF and yield stable ternary compounds. The generic LiF-scavenging reaction of a fluoride M_xF can be written as,

$$aM_xF + LiF \rightarrow (M_xF)_a\,(LiF) \tag{15}$$

An exhaustive search for LiF scavengers requires a large database of ternary $(M_xF)_a$(LiF) compounds in all Li-M-F systems. However, the number of known Li-M-F compounds available in the ICSD is already very limited. To predict new ternary compounds, one would need to carry out a massive set of DFT calculations even for a single Li-M-F system (e.g., see ref. [46]

© 2014 WILEY-VCH Verlag GmbH & Co. KGaA, Weinheim

AMPEREX Ex. 1024
Page 8
16146840, 2014, 17, Downloaded from https://onlinelibrary.wiley.com/doi/10.1002/aenm.201400690 by Jennifer Babbitt , Wiley Online Library on [05/05/2023]. See the Terms and Conditions (https://onlinelibrary.wiley.com/terms-and-conditions) on Wiley Online Library for rules of use; OA articles are governed by the applicable Creative Commons License

16146840, 2014, 17, Downloaded from https://onlinelibrary.wiley.com/doi/10.1002/aenm.201400690 by Jennifer Babbitt , Wiley Online Library on [05/05/2023]. See the Terms and Conditions (https://onlinelibrary.wiley.com/terms-and-conditions) on Wiley Online Library for rules of use; OA articles are governed by the applicable Creative Commons License

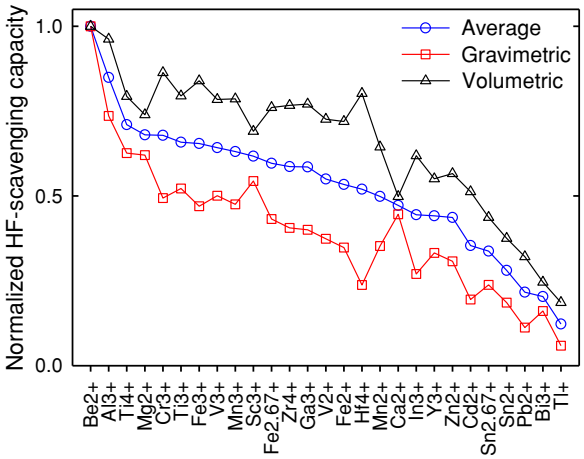

Figure 6. Coating candidates that pass the applied screens versus their normalized HF-scavenging capacities. Averages of the normalized scavenging capacities are also shown. Compounds are labeled with their cations for simplicity.

for the Li-Fe-F system), and such a high-throughput structure prediction is beyond the scope of this work. Here, we simply introduce the LiF-scavenging concept, and we instead utilize the ternary Li-M-F compounds available in the ICSD. The enumerated LiF-scavenging reactions and their enthalpies ($\Delta H_{s-\mathrm{LiF}}$) are listed in Table 3.

In support of the existence of a LiF-scavenging mechanism, a phase in the form $(M_xF)_a(LiF)$ was observed by Liu et al.[86] when nano-Al_2O_3 was soaked in a $LiPF_6$ based electrolyte. They identified reactions that involve HF and LiF, and lead to AlF_3 and Li_3AlF_6 formation on the cathode surfaces. This validates our prediction (Table 3) of the stability of Li_3AlF_6 with respect to AlF_3 and LiF; i.e., AlF_3 can react with LiF to produce Li_3AlF_6. Sun and co-workers[39] also proposed that AlF_3 may be reducing the LiF precipitation on $LiCoO_2$. Moreover, LiF formation was observed to be significantly retarded in presence of a TiO_2 coating,[33] in accord with our prediction (Table 3) of the stability of Li_2TiF_6. Our hypothesis, therefore, is supported by experimental observations. LiF-scavenging can be an important mechanism which contributes to the performance of coatings like Al_2O_3, ZrO_2 and TiO_2 (and their fluoride counterparts). Among the compounds that are already tested experimentally or those we have indicated to be promising, Al^{3+}, Be^{2+}, Cr^{3+}, Ga^{3+}, Mn^{3+}, Nb^{5+}, Pt^{4+}, Ta^{5+}, Ti^{4+}, Y^{3+} and Zr^{4+} oxides/fluorides can potentially reduce LiF-precipitation on cathode particles by forming stable ternary Li-M-F compounds, as listed in Table 3.

3.5. Beyond the Current Thermodynamic Framework

Our analysis in the preceding sections focuses on the important phenomena of HF-scavenging, Li-loss into components of a coating and LiF-scavenging concept, which are mainly related to the thermodynamic mechanisms of cathode protection by coatings. In this section, we discuss the limitations of the current framework and suggest possible future studies that can help further understand the cathode protection mechanisms.

The forms of the reactions given in Equation (4), (7), (8) and (15) are assumed in accordance with the experimental observations. The actual reaction paths may exhibit intermediate steps involving ternary or quaternary compounds such as metal-oxyfluorides, -hydroxides or other metal-complexes, with or without lithium. For instance, hydration of coatings can be important to overcome the water regeneration issue[24] in Equation (4), since it causes further acid production. Also, we consider lithiation to occur by the reactions in Equation (7) and (8) which give average voltages, whereas the actual lithiation path may involve ternary Li-M-F compounds or Li insertion. Such intermediate steps of reactions should be explored for specific cathode coatings in future studies. In addition, although we select fluorides as the products of HF-scavenging reactions, there are a large variety of anions other than F^- in the electrolyte that a metal cation can bind to, such as $(OH)^-$, PF_6^- or $(CO_3)^{2-}$, etc. However, to incorporate such anions into the thermodynamic framework requires knowledge of the activities of these ions in the electrolyte, which are not always readily available. In summary, all reactions we consider are measures of the overall processes, biased by the selection of the reactants and products according to the experimental observations. Nevertheless, the selected reactions yield results consistent with the experimental capacity retentions, as we have shown in previous sections.

Our screening methodology is based on bulk thermodynamic aspects to reveal the general trend among various HF-scavenger coating candidates, but the actual performance of the coating can depend on additional factors such as the cathode material, as well as uniformity, morphology and thickness of the coating. The specific criteria we give here for HF scavenging energies and lithiation voltages may need adjustments for a particular cathode material. Complete surface coverage with compounds stable against acids may provide adequate physical protection, while the HF-scavenging mechanism is suggested to be of particular importance when coatings are rough or patchy.[15] Coatings or subsequently formed layers may also be amorphous.[90] However, we do not expect the slightly higher energies of amorphous phases to significantly alter the thermodynamic tendencies revealed here. In contrast, we note that kinetic properties such as Li^+ or e- transport may be significantly affected by the degree of crystallinity of the material.[90] Ensuring uninterrupted Li^+ transport through the coating components is a key factor in designing coatings that do not diminish the rate capability of a Li-ion battery. Computational investigation of such kinetic processes, however, is often an intricate task that requires focusing on a smaller set of materials than we consider in this work. Therefore, our work serves as an initial discussion of the thermodynamics of a particular failure mechanism, i.e., that of HF attack, and identifies the thermodynamically promising materials prior to kinetic investigations, which will be the subject of future studies.

It is also important that both reactants and products are stable solids in the presence of electrolytes and at operating temperatures of Li-ion batteries. For example, we have already taken into account during screening that although they can scavenge HF, materials such as SiO_2, B_2O_3, Nb_2O_5 or Ta_2O_5 are likely to have performances inferior to other candidates due to unstable or low melting point fluorides at operating temperatures. A different example is the LiF-scavenging product

© 2014 WILEY-VCH Verlag GmbH & Co. KGaA, Weinheim

AMPEREX Ex. 1024
Page 9

Table 3. LiF-scavenging reactions and enthalpies calculated with DFT. In Li-Cs-F system, we only list two reactions and do not further list those for $LiCs_2F_3$, Li_2CsF_3, Li_3CsF_4 and $Li_3Cs_2F_5$ since none of them are stable with respect to CsF and LiF.

Reaction	ΔH_{s-LiF} [eV LiF^{-1}]	Reaction	ΔH_{s-LiF} [eV LiF^{-1}]
$AlF_3 + 3LiF \rightarrow Li_3AlF_6$	–0.118	$MnF_3 + LiF \rightarrow LiMnF_4$	–0.096
$AsF_5 + LiF \rightarrow LiAsF_6$	–0.938	$LiMnF_4 + LiF \rightarrow Li_2MnF_5$	–0.009
$AuF_3 + LiF \rightarrow LiAuF_4$	–0.524	$MnF_4 + 2LiF \rightarrow Li_2MnF_6$	–0.395
$AuF_5 + LiF \rightarrow LiAuF_6$	–1.050	$NbF_4 + 2LiF \rightarrow Li_2NbF_6$	–0.147
$BaF_2 + LiF \rightarrow LiBaF_3$	0.118	$NbF_5 + LiF \rightarrow LiNbF_6$	–0.736
$BeF_2 + 2LiF \rightarrow Li_2BeF_4$	–0.125	$PdF_4 + 2LiF \rightarrow Li2PdF_6$	–0.609
$BiF_3 + LiF \rightarrow LiBiF_4$	–0.142	$PtF_4 + 2LiF \rightarrow Li_2PtF_6$	–0.665
$BiF_5 + LiF \rightarrow LiBiF_6$	–0.856	$RbF + LiF \rightarrow LiRbF_2$	–0.070
$CoF_3 + LiF \rightarrow LiCoF_4$	–0.083	$RuF_4 + 2LiF \rightarrow Li_2RuF_6$	–0.143
$CrF_3 + 3LiF \rightarrow Li_3CrF_6$	–0.136	$ScF_3 + 3LiF \rightarrow Li_3ScF_6$	0.018
$CrF_4 + 2LiF \rightarrow Li_2CrF_6$	–0.404	$TaF_5 + LiF \rightarrow LiTaF_6$	–0.877
$CsF + LiF \rightarrow LiCsF_2$	–0.017	$TiF_4 + 2LiF \rightarrow Li_2TiF_6$	–0.731
$3CsF + LiF \rightarrow LiCs_3F_4$	0.087	$YF_3 + LiF \rightarrow LiYF_4$	–0.207
$GaF_3 + 3LiF \rightarrow Li_3GaF_6$	–0.153	$ZrF_4 + 2LiF \rightarrow Li_2ZrF_6$	–0.246
$GeF_4 + 2LiF \rightarrow Li_2GeF_6$	–0.545	$Li_2ZrF_6 + 2LiF \rightarrow Li_4ZrF_8$	–0.008
$InF_3 + LiF \rightarrow LiInF_4$	–0.102		

$LiAsF_6$, which is already known to be a salt for Li-ion battery electrolytes, and may tend to dissolve in the electrolyte. Furthermore, it must be ensured that the Li^+ and e- conductivity of the products of LiF-scavenging reactions are superior to LiF itself. Finally, there are also other qualities expected from a coating, such as good adhesion to cathode surface, cost-effectiveness, and more importantly good Li^+ and e- conductivity, which we do not take into account in our thermodynamic analysis.

4. Conclusion

In this study, we have introduced a thermodynamic framework for screening cathode coating materials for Li-ion batteries with HF-bearing electrolytes. The framework is based on four attributes: i) HF-scavenging tendencies, ii) volumetric and iii) gravimetric HF-scavenging capacities of oxides, and iv) tendencies of cyclable-Li loss into components (oxides and fluorides) of the evolving coating. Of the 81 HF-scavenging reactions enumerated among the s-, p- and d-block binary metal oxides and fluorides, about half of the reactions lack enough experimental thermochemical data to calculate reaction energies, and the majority of the rest have large combined standard uncertainties. Employing DFT-based thermodynamics, we have conducted a systematic analysis of binary oxide/fluoride coating candidates by incorporating all four attributes (i-iv) in a combinatorial design scheme. We have demonstrated that some of the cyclable-Li might be lost into metal fluorides, due to their lithiation voltages being around 1.0 to 1.5 V higher than the corresponding oxides. The enhancements in capacity retention observed in experiments when the cathode particles are coated with metal oxides such as Al_2O_3, ZrO_2, TiO_2 or MgO are found to be consistent with the current thermodynamic design approach. Further comparison of our results for p-block compounds with experimental data helped us demonstrate that HF-scavenging is effective only when a solid fluoride layer can form as a product of the HF-scavenging reaction. While Al_2O_3 –the most widely studied cathode coating– and MgO outperform most of the p- and d-block compounds, trivalent d-block oxides Sc_2O_3, Ti_2O_3, V_2O_3, Cr_2O_3, Mn_2O_3 and Y_2O_3 are predicted to be competitive coatings. Design attributes (i-iv) of these materials are closer to Al_2O_3 and MgO than the rest of the p- or d-block metal oxides. Furthermore, we have shown that LiF-scavenging might be one of the protection mechanisms that successful coatings exhibit. The current DFT-based approach can reduce the experimental efforts required to discover novel coating materials optimized for systems with an $LiPF_6$-based electrolyte and residual water (where HF-attack can be a degradation mechanism), when combined with information regarding kinetic and electronic aspects; namely, ionic and electronic conductivities of the components of a coating.

Supporting Information

Supporting Information is available from the Wiley Online Library or from the author.

Acknowledgements

M.A. and C.W. were supported by The Dow Chemical Company. S.K. was supported by the Center for Electrical Energy Storage (CEES), an Energy Frontier Research Center funded by the US Department of Energy, Office of Science and Office of Basic Sciences. The authors also gratefully acknowledge helpful discussions with Dr. Shiqiang Hao, Dr. Jishnu Bhattacharya and David Snydacker.

Received: April 24, 2014
Revised: June 11, 2014
Published online: August 5, 2014

[1] J. Vetter, P. Novák, M. R. Wagner, C. Veit, K.-C. Möller, J. O. Besenhard, M. Winter, M. Wohlfahrt-Mehrens, C. Vogler, A. Hammouche, *J. Power Sources* **2005**, *147*, 269.
[2] M. M. Thackeray, C. Wolverton, E. D. Isaacs, *Energy Environ. Sci.* **2012**, *5*, 7854.
[3] G. Amatucci, J. Tarascon, L. Klein, *Solid State Ionics* **1996**, *83*, 167.
[4] K. Edstrom, T. Gustafsson, J. Thomas, *Electrochim. Acta* **2004**, *50*, 397.
[5] S. E. Sloop, J. K. Pugh, S. Wang, J. B. Kerr, K. Kinoshita, *Electrochem. Solid-State Lett.* **2001**, *4*, A42.
[6] T. Kawamura, S. Okada, J. Yamaki, *J. Power Sources* **2006**, *156*, 547.
[7] C. L. Campion, W. Li, B. L. Lucht, *J. Electrochem. Soc.* **2005**, *152*, A2327.
[8] T. Stoebe, R. Huggins, *J. Mater. Sci.* **1966**, *1*, 117.
[9] K. Tasaki, A. Goldberg, J.-J. Lian, M. Walker, A. Timmons, S. J. Harris, *J. Electrochem. Soc.* **2009**, *156*, A1019.
[10] W. Strehlow, E. Cook, *J. Phys. Chem. Ref. Data* **1973**, *2*, 163.
[11] E. Markevich, G. Salitra, D. Aurbach, *Electrochem. Commun.* **2005**, *7*, 1298.
[12] D. Aurbach, Y. Talyosef, B. Markovsky, E. Markevich, E. Zinigrad, L. Asraf, J. S. Gnanaraj, H.-J. Kim, *Electrochim. Acta* **2004**, *50*, 247.

© 2014 WILEY-VCH Verlag GmbH & Co. KGaA, Weinheim

AMPEREX Ex. 1024
Page 10

16146840, 2014, 17, Downloaded from https://onlinelibrary.wiley.com/doi/10.1002/aenm.201400690 by Jennifer Babbitt , Wiley Online Library on [05/05/2023]. See the Terms and Conditions (https://onlinelibrary.wiley.com/terms-and-conditions) on Wiley Online Library for rules of use; OA articles are governed by the applicable Creative Commons License

16146840, 2014, 17, Downloaded from https://onlinelibrary.wiley.com/doi/10.1002/aenm.201400690 by Jennifer Babbitt , Wiley Online Library on [05/05/2023]. See the Terms and Conditions (https://onlinelibrary.wiley.com/terms-and-conditions) on Wiley Online Library for rules of use; OA articles are governed by the applicable Creative Commons License

[13] Y.-K. Sun, M.-J. Lee, C. S. Yoon, J. Hassoun, K. Amine, B. Scrosati, *Adv. Mater.* **2012**, *24*, 1192.
[14] J. Cho, Y. J. Kim, B. Park, *Chem. Mater.* **2000**, *4*, 3788.
[15] Z. Chen, Y. Qin, K. Amine, Y.-K. Sun, *J. Mater. Chem.* **2010**, *20*, 7606.
[16] S. Myung, K. Izumi, S. Komaba, H. Yashiro, H. J. Bang, Y.-K. Sun, N. Kumagai, *J. Phys. Chem. C* **2007**, *111*, 4061.
[17] Z. Chen, D.-J. Lee, Y.-K. Sun, K. Amine, *MRS Bull.* **2011**, *36*, 498.
[18] N. Van Landschoot, E. M. Kelder, P. J. Kooyman, C. Kwakernaak, J. Schoonman, *J. Power Sources* **2004**, *138*, 262.
[19] S. Myung, K. Izumi, S. Komaba, Y. Sun, *Chem. Mater.* **2005**, *17*, 3695.
[20] Z. Wang, L. Liu, L. Chen, X. Huang, *Solid State Ionics* **2002**, *148*, 335.
[21] J. Cho, Y. J. Kim, T.-J. Kim, B. Park, *Angew. Chemie* **2001**, *40*, 3367.
[22] J. Cho, T.-G. Kim, C. Kim, J.-G. Lee, Y.-W. Kim, B. Park, *J. Power Sources* **2005**, *146*, 58.
[23] Y. J. Kim, J. Cho, T.-J. Kim, B. Park, *J. Electrochem. Soc.* **2003**, *150*, A1723.
[24] J.-S. Kim, C. S. Johnson, J. T. Vaughey, S. A. Hackney, K. A. Walz, W. A. Zeltner, M. A. Anderson, M. M. Thackeray, *J. Electrochem. Soc.* **2004**, *151*, A1755.
[25] Y.-C. Lu, A. N. Mansour, N. Yabuuchi, Y. Shao-Horn, *Chem. Mater.* **2009**, *21*, 4408.
[26] Y. Wang, G. Cao, *Adv. Mater.* **2008**, *20*, 2251.
[27] G. Li, Z. Yang, W. Yang, *J. Power Sources* **2008**, *183*, 741.
[28] H. ahan, H. Göktepe, . Patat, *J. Mater. Sci. Technol.* **2011**, *27*, 415.
[29] S. B. Jang, S.-H. Kang, K. Amine, Y. C. Bae, Y.-K. Sun, *Electrochim. Acta* **2005**, *50*, 4168.
[30] Y. Sun, K. Hong, J. Prakash, K. Amine, *Electrochem. Commun.* **2002**, *4*, 344.
[31] X. Cao, L. Guo, J. Liu, L. Xie, *Int. J. Electrochem. Sci.* **2011**, *6*, 270.
[32] G. T. -K. Fey, C.-Z. Lu, J.-D. Huang, T. P. Kumar, Y.-C. Chang, *J. Power Sources* **2005**, *146*, 65.
[33] J. M. Zheng, J. Li, Z. R. Zhang, X. J. Guo, Y. Yang, *Solid State Ionics* **2008**, *179*, 1794.
[34] H. Zhao, L. Gao, W. Qiu, X. Zhang, *J. Power Sources* **2004**, *132*, 195.
[35] E. Zhecheva, R. Stoyanova, G. Tyuliev, K. Tenchev, M. Mladenov, S. Vassilev, *Solid State Sci.* **2003**, *5*, 711.
[36] J. Zhai, M. Zhao, D. Wang, Y. Qiao, *J. Alloys Compd.* **2010**, *502*, 401.
[37] W.-S. Yoon, K.-W. Nam, D. Jang, K. Y. Chung, J. Hanson, J.-M. Chen, X.-Q. Yang, *J. Power Sources* **2012**, *217*, 128.
[38] H. Şahan, H. Göktepe, Ş. Patat, A. Ülgen, *Solid State Ionics* **2010**, *181*, 1437.
[39] Y. Sun, J. Han, S. Myung, S. Lee, K. Amine, *Electrochem. Commun.* **2006**, *8*, 821.
[40] S. Myung, K. Lee, C. S. Yoon, Y. Sun, K. Amine, H. Yashiro, *J. Phys. Chem. C* **2010**, *114*, 4710.
[41] J.-H. Kim, M.-S. Park, J.-H. Song, D.-J. Byun, Y.-J. Kim, J.-S. Kim, *J. Alloys Compd.* **2012**, *517*, 20.
[42] K. Xu, Z. Jie, R. Li, Z. Chen, S. Wu, J. Gu, J. Chen, *Electrochim. Acta* **2012**, *60*, 130.
[43] H. G. Song, S. B. Kim, Y. J. Park, *J. Electroceramics* **2012**, *29*, 163.
[44] K. Amine, J. Liu, I. Belharouak, S.-H. Kang, I. Bloom, D. Vissers, G. Henriksen, *J. Power Sources* **2005**, *146*, 111.
[45] J. Cabana, L. Monconduit, D. Larcher, M. R. Palacín, *Adv. Mater.* **2010**, *22*, E170.
[46] F. Wang, H.-C. Yu, M.-H. Chen, L. Wu, N. Pereira, K. Thornton, A. Van der Ven, Y. Zhu, G. G. Amatucci, J. Graetz, *Nat. Commun.* **2012**, *3*, 1201.
[47] M. W. Chase, C. A. Davies, J. R. Downey, D. J. Frurip, R. A. McDonald, A. N. Syverud, *J. Phys. Chem. Ref. Data.* **1985**, *14*, Suppl. 1.
[48] O. Kubaschewski, C. B. Alcock, P. J. Spencer, *Materials Thermochemistry*, 6th ed., Pergamon Press, Oxford **1993**.
[49] I. Barin, *Thermochemical Data of Pure Substances*, 3rd ed., VCH, Weinheim **1995**.
[50] M. Aydinol, G. Ceder, *J. Electrochem. Soc.* **1997**, *144*, 3832.
[51] M. Aydinol, A. Kohan, G. Ceder, K. Cho, J. Joannopoulos, *Phys. Rev. B* **1997**, *56*, 1354.
[52] C. Wolverton, A. Zunger, *Phys. Rev. Lett.* **1998**, *81*, 606.
[53] C. Wolverton, A. Zunger, *J. Electrochem. Soc.* **1998**, *145*, 2424.
[54] G. Ceder, G. Hautier, A. Jain, S. P. Ong, *MRS Bull.* **2011**, *36*, 185.
[55] S. Kirklin, B. Meredig, C. Wolverton, *Adv. Energy Mater.* **2013**, *3*, 252.
[56] S. P. Ong, O. Andreussi, Y. Wu, N. Marzari, G. Ceder, *Chem. Mater.* **2011**, *23*, 2979.
[57] Y. S. Meng, M. E. Arroyo-de Dompablo, *Energy Environ. Sci.* **2009**, *2*, 589.
[58] M. K. Y. Chan, C. Wolverton, J. P. Greeley, *J. Am. Chem. Soc.* **2012**, *134*, 14362.
[59] J. Bhattacharya, C. Wolverton, *Phys.Chem. Chem. Phys.* **2013**, *15*, 6486.
[60] S. Curtarolo, G. L. W. Hart, M. B. Nardelli, N. Mingo, S. Sanvito, O. Levy, *Nat. Mater.* **2013**, *12*, 191.
[61] R. Benedek, A. van de Walle, *J. Electrochem. Soc.* **2008**, *155*, A711.
[62] R. Marom, S. F. Amalraj, N. Leifer, D. Jacob, D. Aurbach, *J. Mater. Chem.* **2011**, *21*, 9938.
[63] J. C. Hunter, *J. Solid State Chem.* **1981**, *39*, 142.
[64] D. Aurbach, B. Markovsky, A. Rodkin, E. Levi, Y. S. Cohen, H.-J. Kim, M. Schmidt, *Electrochim. Acta* **2002**, *47*, 4291.
[65] G. Kresse, J. Hafner, *Phys. Rev. B* **1993**, *47*, 558.
[66] G. Kresse, J. Hafner, *Phys. Rev. B* **1994**, *49*, 14251.
[67] G. Kresse, J. Furthmüller, *Comput. Mater. Sci.* **1996**, *6*, 15.
[68] G. Kresse, J. Furthmüller, *Phys. Rev. B* **1996**, *54*, 11169.
[69] P. E. Blöchl, *Phys. Rev. B* **1994**, *50*, 17953.
[70] J. P. Perdew, K. Burke, M. Ernzerhof, *Phys. Rev. Lett.* **1996**, *77*, 3865.
[71] J. P. Perdew, K. Burke, M. Ernzerhof, *Phys. Rev. Lett.* **1997**, *78*, 1396.
[72] S. Dudarev, G. Botton, S. Savrasov, C. Humphreyes, A. Sutton, *Phys. Rev. B* **1998**, *57*, 1505.
[73] L. Wang, T. Maxisch, G. Ceder, *Phys. Rev. B* **2006**, *73*, 1.
[74] A. Belsky, M. Hellenbrandt, V. L. Karen, P. Luksch, *Acta Crystallogr. Sect. B Struct. Sci.* **2002**, *58*, 364.
[75] J. E. Saal, S. Kirklin, B. Meredig, J. Doak, A. Thompson, S. Ruehl, C. Wolverton, **2013**, unpublished.
[76] J. E. Saal, S. Kirklin, M. Aykol, B. Meredig, C. Wolverton, *JOM* **2013**, *65*, 1501.
[77] S. Grindy, B. Meredig, S. Kirklin, J. Saal, C. Wolverton, *Phys. Rev. B* **2013**, *87*, 075150.
[78] G. K. Johnson, *J. Chem. Thermodyn.* **1981**, *13*, 465.
[79] A. M. Azad, O. M. Sreedharan, *J. Appl. Electrochem.* **1987**, *17*, 949.
[80] T. C. Ehlert, M. Hsia, *J. Fluor. Chem.* **1972**, *2*, 33.
[81] K. Jacob, J. Hajra, *Bull. Mater. Sci.* **1987**, *9*, 37.
[82] Y. Koyama, I. Tanaka, H. Adachi, *J. Electrochem. Soc.* **2000**, *147*, 3633.
[83] A. R. Akbarzadeh, V. Ozoliņš, C. Wolverton, *Adv. Mater.* **2007**, *19*, 3233.
[84] T. H. Mason, X. Liu, J. Hong, J. Graetz, E. H. Majzoub, *J. Phys. Chem. C* **2011**, *115*, 16681.
[85] W. Q. Sun, C. Wolverton, A. R. Akbarzadeh, V. Ozolins, *Phys. Rev. B* **2011**, *83*, 064112.
[86] J. Liu, N. Liu, D. Liu, Y. Bai, L. Shi, Z. Wang, L. Chen, V. Hennige, A. Schuch, *J. Electrochem. Soc.* **2007**, *154*, A55.
[87] C. Cárdenas, F. De Proft, E. Chamorro, P. Fuentealba, P. Geerlings, *J. Chem. Phys.* **2008**, *128*, 034708.
[88] J. Cho, J. Lee, B. Kim, B. Park, *Chem. Mater.* **2003**, 3190.
[89] Y. Bai, F. Wu, H. T. Yang, Y. Zhong, C. Wu, *Adv. Mater. Res.* **2011**, *391–392*, 1069.
[90] S. Hao, C. Wolverton, *J. Phys. Chem. C* **2013**, *117*, 8009.

© 2014 WILEY-VCH Verlag GmbH & Co. KGaA, Weinheim